

# Zn Impurities in $\text{Bi}_2\text{Sr}_2\text{Ca}(\text{Cu}_{1-x}\text{Zn}_x)_2\text{O}_{8+\delta}(\text{I})$ - Electronic Structure Evolution

P.J. White<sup>(1)</sup>, Z.-X. Shen<sup>(1)</sup>, D.L. Feng<sup>(1)</sup>, C. Kim<sup>(1)</sup>, M.-Z. Hasan<sup>(1)</sup>, J.M. Harris<sup>(1)</sup>, A.G. Loeser<sup>(1)</sup>, H. Ikeda<sup>(2)</sup>,  
R. Yoshizaki<sup>(2)</sup>, G.D. Gu<sup>(3)</sup>, N. Koshizuka<sup>(4)</sup>

<sup>(1)</sup> *Department of Applied Physics and Stanford Synchrotron Radiation Laboratory, Stanford University, Stanford, CA 94305-4045*

<sup>(2)</sup> *Institute of Applied Physics and Cryogenics Center, University of Tsukuba, Tsukuba, Ibaraki 305 Japan*

<sup>(3)</sup> *School of Physics, The University of New South Wales, PO Box 1, Kensington, N.S.W. 2033*

<sup>(4)</sup> *Superconductivity Research Laboratory, ISTEC, 10-13 Shinonome, 1-Chome, Koto-Ku, Tokyo 135, Japan*

A small amount of Zn substitution for Cu essentially washes out the otherwise sharp spectral peak along the  $(0,0)$  to  $(\pi, \pi)$  direction in  $\text{Bi}_2\text{Sr}_2\text{Ca}(\text{Cu}_{1-x}\text{Zn}_x)_2\text{O}_{8+\delta}$ , while superconductivity with  $T_c$  as high as 78-83K survives. This behavior contrasts markedly from that seen in cases where the impurities are located off the  $\text{CuO}_2$  plane, as well as when the  $\text{CuO}_2$  planes are underdoped. This effect is also accompanied by changes of low energy excitations at  $(\pi, 0)$ , near the anti-node position of the  $d_{x^2-y^2}$  pairing state. With Zn doping the size of the superconducting gap is significantly suppressed, the width of the quasiparticle peak in the superconducting state becomes wider, and the dip at higher binding energy is diminished.

PACS:71.20.-b,71.27.+a,74.25.Jb

## I. INTRODUCTION

Impurity doping has been a very effective tool to probe the properties of cuprate superconductors. In particular, Zn substitution of Cu in the  $\text{CuO}_2$  planes is known to depress  $T_c$  [1] - [6]. An extensive amount of experiments have been conducted to understand the effect of Zn doping, including specific heat, microwave, NMR,  $\mu\text{SR}$ , optical, neutron, and tunnelling experiments [7] - [20]. Transport and microwave experiments indicate that Zn is a very strong scatterer, resulting in a strong increase in the residual resistivity in the plane [3] [4] [12]. A similar conclusion was drawn from  $\mu\text{SR}$  experiments, which also found that Zn suppresses the superfluid density [15]. Specific heat, transport, and optical experiments indicate Zn doping alters the residual density of states and affects the low energy charge dynamics [10] - [13] [21]. NMR and neutron experiments generally show that Zn introduces low lying excitations in the spin channel [16] - [19] and dramatically affects the dynamical spin fluctuations. In particular, the NMR experiments show that Zn induces local magnetic moments in the normal state that do not otherwise show local moment behavior.

More recently, Zn doping is also found to enhance the  $T_c$  suppression and other anomalies near  $\frac{1}{8}$  doping in  $\text{La}_{2-x}\text{Sr}_x\text{CuO}_4$  (LSCO),  $\text{YBa}_2\text{Cu}_3\text{O}_7$  (YBCO), and Y doped  $\text{Bi}_2\text{Sr}_2\text{CaCu}_2\text{O}_{8+\delta}$  [22]. This later result has been speculated to be the charge stripe instability [22], similar to a possible interpretation of neutron data from LSCO. In addition, a new neutron scattering experiment has shown two aspects of Zn doping. First, it found that Zn shortens the correlation length of the static spin density wave [20]. Second, it found that the Zn shifts the spectral weight to lower energy, a fact consistent with the idea that Zn serves to stabilize a short range order incommensurate spin density wave state which might otherwise be

purely dynamic [16] [20].

It is thus desirable to further investigate the Zn impurity effect by directly probing its electronic structure using angle resolved photoemission spectroscopy (ARPES). Over the last decade ARPES has played an important role in advancing our understanding of the low energy single particle excitations in these novel superconductors, starting with the observation of band like features [23]. Most notably, ARPES facilitated the observation of the d-wave superconducting gap structure as well as the normal state pseudogap [24] [25] [26] [27]. Several groups have attempted to study the impurity doping effects using ARPES. Quitmann *et al.* [29] have performed room temperature ARPES of Ni and Co doped  $\text{Bi}2212$  to address the change of the electronic structure in the normal state but not the changes in the superconducting state. Gu *et al.* [30] have attempted to study Zn and Co doped YBCO for which the superconducting property of the  $\text{CuO}_2$  planes is complicated by the surface chain signal [31].

In this paper we report detailed results of ARPES on the nature of the Zn doping effect in the  $\text{Bi}_2\text{Sr}_2\text{Ca}(\text{Cu}_{1-x}\text{Zn}_x)_2\text{O}_{8+\delta}$  system. We found significant changes in the electronic structure near the Fermi level with a small amount of Zn doping. Along the  $(0,0)$  to  $(\pi, \pi)$  direction, Zn doping essentially wiped out the otherwise well defined quasiparticle peak [32] in samples with  $T_c$  as high as 78-83K. This behavior contrasts strongly to the case where scattering impurities are located off the  $\text{CuO}_2$  plane as well as to the case of an underdoped  $\text{CuO}_2$  plane. Zn doping also causes a systematic change of data near  $(\pi, 0)$ , which is close to the anti-node region of the d-wave pairing state. Indeed, the superconducting gap is decreased as one would expect from pair breaking considerations. At the same time, the dip seems almost gone in  $\text{Bi}_2\text{Sr}_2\text{Ca}(\text{Cu}_{1-x}\text{Zn}_x)_2\text{O}_{8+\delta}$ . This suggests an interesting

evolution of the  $(\pi, 0)$  superconducting spectrum as the traditionally two distinct features (the broad incoherent peak and the sharp quasiparticle peak) seem to evolve differently with Zn doping.

This paper is organized into several parts: Experimental (II); Experimental Observation (III); and Discussion and Conclusion (IV). Part II will give a brief description of the experimental apparatus. Part III will note our observations in different doping studies for different temperatures and  $\mathbf{k}$ -space positions. Finally, Part IV will attempt to elucidate our observations in light of recent theory and experiments.

## II. EXPERIMENTAL

Single crystals of  $\text{Bi}_2\text{Sr}_2\text{CaCu}_2\text{O}_{8+\delta}$  (Bi2212) and  $\text{Bi}_2\text{Sr}_2\text{Ca}(\text{Cu}_{1-x}\text{Zn}_x)_2\text{O}_{8+\delta}$  (Zn doped Bi2212) were prepared using a traveling solvent floating zone method [33] [34]. These crystals were characterized according to  $T_c$  and the Zn concentration, which was determined by electron probe microanalysis (EPMA). The crystals were grown under the nominal condition to produce optimal doping, with  $T_c$  of the pure and Zn doped samples ranging from 91K to 78K, as shown in Fig. 1. The transition widths vary from 3-5K according to susceptibility measurements, indicating the high quality of these crystals. The single phase of the samples was verified by X-ray scattering. X-ray rocking curves indicate that the crystalline quality of the Zn doped Bi2212 is comparable to that of the pure Bi2212. In this paper, we report results from samples of 0.6% to 0.9% Zn doping. The amount of Zn at each exposed surface is not uniform, as revealed by the varying signal intensities near the Zn 3d core level energy as well as variations in the spectra. We organize our results according to the intensity of the Zn 3d core level region. The data presented here are from surfaces with clearly detectable Zn 3d signals. Although we do not know quantitatively the amount of Zn at the surfaces studied, the relative intensity variation of the Zn 3d core level from cleave to cleave suggests that we have up to a factor of 3 variation of Zn content. Another point is that the Zn tends to bring in excess oxygen [1]. However, we have taken data from samples with spectra indicating varying doping concentration, and we see a consistent result.

ARPES spectra were recorded with a VSW chamber attached to beamline 5-3 of the Stanford Synchrotron Radiation Laboratory. The total energy resolution was typically 35meV and 20meV for the data in Fig. 3, and the angular resolution was  $\pm 1$  degree, corresponding to a  $\mathbf{k}$ -space window of  $0.045\frac{\pi}{a}$  or  $0.0037\text{\AA}^{-1}$ . The nominal chamber pressure during the measurement was  $2 \times 10^{-11}$  torr and the photon energy used was 22.4eV. At this photon energy an ARPES spectrum mimics the spectral

function,  $A(\mathbf{k}, \omega)$  [35], weighted by the appropriate factors, such as matrix elements and the Fermi function. Spectra reported here were taken within 10-12 hours of cleaving so as to minimize aging effects as previously reported [24] [36]. This dictates that we can only take selected  $\mathbf{k}$  points in order to have spectra with low enough statistical noise to identify subtle changes in the line-shape; this was critical for data analysis. The flatness of the surfaces of both pure and Zn doped samples was verified by laser reflection patterns after the samples were cleaved *in situ*. Fermi levels were determined by a gold reference sample in electrical contact to the Bi2212 samples.

## III. EXPERIMENTAL OBSERVATION

Figures 2a-f present data at selected  $\mathbf{k}$ -space points along  $(0, 0)$  to  $(\pi, \pi)$  cut ( $\Gamma Y$ ) from pure and Zn doped samples. These points were chosen for their proximity to the Fermi surface and were spaced sufficiently in momentum to reveal the behavior of the Fermi level crossing. For data from pure samples in Fig. 2a-b, we see a relatively sharp feature disperse across  $E_f$  in the expected way. As the peak gets closer to the Fermi level, it apparently narrows in width and, at some point, loses intensity until it ultimately vanishes. This observation is consistent with previous work [23] [25] [26] [27], and much of the peak width is attributable to angular resolution and energy resolution. This general behavior is qualitatively what one expects of a quasiparticle. For data from the Zn doped samples in Figures 2c-d, the dramatic difference is readily apparent. The quasiparticle peak is wiped out with no sharp feature seen at the expected crossing or before it [37].

For comparison, Figures 2e-f reproduce our results from two underdoped samples in similar  $\mathbf{k}$ -space locations [25]. The underdoping in these samples ( $T_c$  near 65K for both) was achieved either by removing oxygen or by substituting 10% Ca by Dy. In both cases the feature along  $\Gamma Y$  remains fairly sharp; this contrasts strongly with data from the Zn doped samples in Fig 2c-d. For the 10% Dy doped sample there is the additional effect of scattering by Dy impurities, whose concentration is much higher than that of the Zn impurities. It is clear that the Zn impurities in the  $\text{CuO}_2$  plane did far more damage to the quasiparticle peak than the more highly concentrated Dy impurities, which are located in the Ca plane sandwiched by the  $\text{CuO}_2$  planes.

Fig 3a shows the  $(\pi, 0)$  spectra of the pure and the Zn doped samples. Unlike the  $\Gamma Y$  line as shown in Fig. 2, the normal state spectra of the pure and Zn doped samples are less different in this region of  $\mathbf{k}$ -space. Both samples show very sharp peaks in the superconducting state. The fact that one can see such a sharp peak below  $T_c$  in Zn doped samples gave us confidence on the intrinsic nature

of the very broad feature in Fig. 2c-d. It is possible that a disordered surface can produce the effect seen in Fig. 2c-d, however the coexistence of a disordered surface and the sharp feature seen in the data at  $(\pi, 0)$  is unlikely.

There are several subtle but important differences between the  $(\pi, 0)$  superconducting spectra for the pure and Zn doped samples. Readily apparent is the fact that there is virtually no dip at the higher binding energy side of the sharp peak in the Zn doped samples, whereas the dip is clearly visible in the pure sample as found before [38] [39]. The superconducting quasiparticle peak is also broader in the Zn doped sample, implying a stronger scattering rate. In the Zn free sample, the peak width is resolution limited. While the spectral weight of the Zn free sample is balanced above and below  $T_c$ , the spectral weight of the Zn doped sample is increased at lower temperature because of the sharp peak's development. Two changes in the spectra contribute to this imbalance: the dip no longer exists and the peak is significantly broadened, even though it has the same relative maximum. The sum rule of  $A(\mathbf{k}, \omega)$  requires spectral weight to come from other locations in energy and/or momentum space.

Another significant observation in Fig. 3a is that the sharp peak in the Zn doped sample shifts to lower binding energy as compared to that of the Zn free sample. This can be interpreted as the size of the superconducting gap being suppressed in the Zn doped sample. In the literature, the size of the energy gap in photoemission is often characterized by the position of the leading edge midpoint in the spectra recorded at the underlying Fermi surface [24] [25] [26] [27]. In this case, because the peak is appreciably broadened in the Zn doped sample, the leading edge analysis is not ideal. We use the quasiparticle peak position as a way to characterize the gap. Although the  $(\pi, 0)$  point is not at the Fermi surface, the band in this region is very flat, and we could use it to characterize the relative change of the gap size [28]. Indeed this notion is confirmed by spectra recorded at  $(\pi, 0.2\pi)$ , which is at the Fermi surface.

The relative changes of the peak in Fig. 3a suggests the superconducting gap is suppressed in the Zn doped samples. Note the difference in the rate of  $\Delta$  suppression and  $T_c$  suppression as a function of Zn doping. It is clear that the gap is severely suppressed in the Zn doped samples, given the modest  $T_c$  decrease at this doping level. This further collaborated our earlier conclusion that  $T_c$  and gap are unrelated energy scales. A possible scenario is that  $T_c$  is not limited by pairing strength but by phase fluctuation effects [40] [41] [42] [43]. It is also worth noting that the normal state spectrum at  $(\pi, 0)$  of the Zn doped sample is cut off by the Fermi function, ruling out the existence of the normal state pseudogap. This is not the case for Zn free  $\text{Bi}_2\text{Sr}_2\text{CaCu}_2\text{O}_{8+\delta}$  in Fig. 3a. This finding can be interpreted as Zn doping suppressing the pseudogap or creating low lying excitation inside the gap as reported by other experiments [17] [18].

Summarizing data from Figs. 2 and 3, we observed correlated changes of the electronic structure as a function of Zn doping: the destruction of the quasiparticle along the  $\Gamma Y$  line; the suppression of the superconducting gap; the broadening of the superconducting peak and the suppression of the dip near  $(\pi, 0)$ .

#### IV. DISCUSSION AND CONCLUSIONS

The experimental data presented in Part III raise several interesting points about impurity doping in the cuprates. The first and foremost has to do with whether the conduction mechanism can be described by quasiparticle dynamics. The dramatic differences in the ARPES data of Fig. 2 with a small amount of doping is unexpected from the doping dependence studies of other materials. Photoemission is a signal averaging experiment and is usually quite insensitive to a small amount of doping change, unlike the case here. In transition metal oxides one usually sees only subtle changes with doping variation up to 10-20% [44]. In ordinary metals like Cu or Al the spectra do not change with a very small amount of impurities. The fact that the spectra recorded in the superconducting state along  $\Gamma Y$  remained very broad is also important (the very sharp peak below  $T_c$  at  $(\pi, 0)$  shows it was not due to a contaminated surface). The magnitude of the change with a relatively small amount of Zn suggests the system may be very close to some kind of instability, and the effect of the Zn impurity is amplified by this intrinsic instability. In Zn free samples the sharp, dispersive feature along the  $\Gamma Y$  direction resembles what one would expect from quasiparticles with well defined  $\mathbf{k}$ , although the feature is still far too broad for this description. On the other hand, Zn-Bi2212 showed that there is no quasiparticle with well defined  $\mathbf{k}$  at all in this direction. Given the modest change of  $T_c$ , the change seen in Fig. 2 is quite remarkable. It suggests that normal state quasiparticles with well defined momentum are not essential for superconductivity. The observed change of the low energy electronic structure in Fig. 2 is consistent with reports from other experiments. NMR, specific heat, microwave, optics, and transport experiments indicate that Zn doping alters the residual density of states [10] - [13] [21] and affects the low energy and spin dynamics [15] - [19]. The  $\mathbf{k}$ -resolved information from ARPES is new.

The second issue is the role of Zn impurities in these superconductors. Naively, one would think that Zn doping causes significant scattering in the  $\text{CuO}_2$  plane, and this would cause an angular averaging effect. To access this possibility we averaged the spectra from the six angles in Fig. 2a, resulting in the top curve in Fig. 2a. Here the *average* of the spectra along  $\Gamma Y$  is plotted. As parallel cuts are similar in the nearby regions, inclusion of these cuts in the averaging process would have a smaller

effect than what we have done here. It is clear that the averaged data still have a sharper structure than those in Fig. 2c-d. Thus, the data in Fig. 2a cannot be explained by a regional averaging effect and a much larger  $\mathbf{k}$ -volume is required to average out the peak if this is the only explanation. The issue is why Zn is such a strong scatterer, as such a small amount of impurity usually causes far less dramatic changes in ordinary materials. Of course, Zn impurities, which are likely to be randomly distributed, will act as strong scatterers themselves. A more interesting question is whether these impurities will induce some collective effects like the ones suggested by neutron experiments. The first collective effect is that Zn impurities induce long range antiferromagnetic order that co-exists with the spin-Peierls transition (seen in in  $\text{Cu}_{1-x}\text{Zn}_x\text{GeO}_3$  [45]) [46] [47]. The second one is that the Zn impurities may pin the dynamical stripes [16] [19].

We will now explore whether this idea provides a self consistent explanation to our data. Specifically, we want to see whether the data are compatible with the idea that Zn impurities pin the dynamical stripes. There are two reasons for us to consider this possibility. The first has to do with transport experiments at  $\frac{1}{8}$  doping [22]. It has been strongly suggested that the  $T_c$  suppression and other transport anomalies at  $\frac{1}{8}$  doping are related to the stripe instability [19]. The work on  $\text{Bi}_2\text{Sr}_2\text{Ca}_{1-x}\text{Y}_x(\text{Cu}_{1-y}\text{Zn}_y)_2\text{O}_{8+\delta}$  is particularly relevant to our discussion here [48]. In Zn doped cases ( $y=0.02-0.03$ ), it is found that the electrical resistivity and thermoelectric power exhibit less metallic behavior than usual near a doping level of  $\frac{1}{8}$ . At the same time,  $T_c$ 's for samples near a doping level of  $\frac{1}{8}$  are also anomalously suppressed. These results suggest that the Zn doped Bi2212 system is rather similar to  $\text{La}_{2-x}\text{Sr}_x\text{CuO}_4$  system and are interpreted as possible evidence that Zn pins the dynamical stripes. The second reason concerns results from neutron experiments. Recent neutron scattering data from  $\text{La}_{2-x}\text{Sr}_x(\text{Cu}_{1-y}\text{Zn}_y)\text{O}_4$  indicate that Zn doping shifts the spectral weight of the incommensurate peaks at  $(\pi, \pi \pm \delta\pi)$  to lower frequencies [16]. As the incommensurate peaks are interpreted as scattering from dynamical stripes [19], the downward shift of spectral weight has been interpreted as stabilization of the dynamic stripes [16]. On the other hand, it is also found that Zn broadened the incommensurate neutron peak, which indicates that Zn doping disrupts the long range order and shortens the correlation length. Hence, it appears that a random distribution of Zn impurities shortens the long range correlation but stabilizes the short range correlation which would otherwise be dynamic [19].

Empirically, ARPES features along (0,0) to  $(\pi, \pi)$  are always sharp, even in underdoped materials (Fig. 2e and Fig. 2f). This is also the case for  $\text{YBa}_2\text{Cu}_3\text{O}_7$  and the Bi2201 systems [49] [50] [51] [31] as well as the insulating  $\text{Sr}_2\text{CuO}_2\text{Cl}_2$  and  $\text{Ca}_2\text{CuO}_2\text{Cl}_2$  [52]. The only cuprate that violates this empirical rule is the  $\text{La}_{2-x}\text{Sr}_x\text{CuO}_4$  sys-

tem. The data from  $\text{La}_{2-x}\text{Sr}_x\text{CuO}_4$  system show strong resemblances to that of the Zn doped system here [53]. In the  $\text{La}_{2-x}\text{Sr}_x\text{CuO}_4$  case spectra along the (0,0) to  $(\pi, \pi)$  direction are found to be extremely broad, while one can still see well defined peaks near  $(\pi, 0)$  for highly doped cases - a fact that shows that the extremely broad feature along the (0,0) to  $(\pi, \pi)$  direction is not due to a bad surface. With the increase of Sr doping, the change of the spectra along (0,0) to  $(\pi, \pi)$  is not monotonic. For  $x < 0.05$ , one sees a broad dispersive feature that behaves like the feature seen in the insulating  $\text{Sr}_2\text{CuO}_2\text{Cl}_2$ . For  $0.05 < x < 0.15$ , one hardly sees any dispersive feature at all. For  $x > 0.2$  one again sees a dispersive feature that shows a clear Fermi level crossing. Hence, the broadness of the feature along (0,0) to  $(\pi, \pi)$  is not simply due to the random disorder of the Sr impurities as the Sr content increases monotonically. There is another likely contribution to the broadness of the features, and the contribution may be connected to the intrinsic electronic inhomogeneity. Based on neutron experiments, the evidence for stripe correlation is strongest in the  $\text{La}_{2-x}\text{Sr}_x\text{CuO}_4$  system and is most visible in the doping range near  $\frac{1}{8}$  [19]. Given the similarity of the data from Zn-Bi2212 and from LSCO, one may wonder whether the destruction of the quasiparticle along (0,0) to  $(\pi, \pi)$  in the Zn samples is also related to the electronic inhomogeneity. This issue is also related to the recent transport measurement on  $\text{Bi}_2\text{Sr}_2\text{Ca}_{1-x}\text{Y}_x(\text{Cu}_{1-y}\text{Zn}_y)_2\text{O}_{8+\delta}$  [48]. We note here that the linear T dependence of the resistivity is basically unchanged with a small amount of Zn doping. The lineshape along (0,0) to  $(\pi, \pi)$  may also be realized in the following fashion: we know that Zn locally alters the magnetic ordering and creates a local antiferromagnetic region around it [8]. This effect serves to enhance the microscopic phase separation. In this way, one can view the effect of photoemission from a microscopically phase separated system as a superposition of photoemission from two separate systems, *i.e.*, the hole rich and the hole poor regions. The low energy excitations relative to the common Fermi level from the hole rich and the hole poor regions are quite different. In this way, there is a 'smearing' of the typical Bi2212 spectra along (0,0) to  $(\pi, \pi)$ . The effect should also occur for the (0,0) to  $(\pi, 0)$ , and, indeed, we have seen some of that in the superconducting spectrum at  $(\pi, 0)$ . However, the reason for the insensitivity along the  $\Gamma\bar{M}$  as compared to along the  $\Gamma\bar{Y}$  direction is not entirely clear.

Extensive numerical calculations using Hubbard or t-J models have been carried out on small cluster samples [54]. The systematics of the spectral lineshapes seen in Bi2212, YBCO,  $\text{Sr}_2\text{CuO}_2\text{Cl}_2$ ,  $\text{Nd}_{2-x}\text{Ce}_x\text{CuO}_4$ , as well as the doping dependence, can very well be accounted for by these calculations. However, the spectral behavior of Zn-Bi2212 and LSCO cannot be explained by these calculations even qualitatively. All calculations produce a sharp structure along (0,0) to  $(\pi, \pi)$ , even when addi-

tional parameters such as  $t'$  and  $t''$  are included [55]. On the other hand, an exact diagonalization of the spectral function shows that an introduction of attractive forces along the (1,0) or (0,1) directions strongly suppresses the quasiparticle-pole strength along (0,0) to (1,1) direction [56]. These forces were introduced to simulate the effects of stripes on the electronic structure, although the origin of stripes is unclear. In another calculation on the t-J model, it is found that a Zn vacancy pins the domain wall, similar to the case where a Zn vacancy bounds a hole of  $d_{x^2-y^2}$  symmetry [57]. Summarizing the above discussion, it appears that the scenario of electronic phase separation can provide a self consistent account for the data. However, the above interpretation is not unique, and the phase separated regions do not have 1D order. Alternatively, the interpretation of the data may come from a more phenomenological viewpoint. It has been stated that Zn has an effect on the electronic properties of the cuprates. One particular result is that Zn induces local moments on neighboring Cu sites [58] [8]. This glassy array of AFM droplets will probably become more ordered as the temperature is lowered [59]. This will have some kind of effect on the electronic structure, and it is possible that the phenomena here are just manifestations of that fact. At the same time, quasiparticles at  $(\frac{\pi}{2}, \frac{\pi}{2})$  will suffer significant scattering, resulting in the washed out features we see here. The spectral lineshape changes at  $(\pi, 0)$  are not surprising as we know Zn is doing something to the superfluid density,  $n_s$ . According to Nachumi *et al.* [60], the Zn impurity acts as a dead center for  $n_s$ . This pocket of no superfluid extends over an area of  $\pi\xi^2$ , where  $\xi$  is the in-plane coherence length. This also says that the volume available for superconductivity is reduced, and this ought to be reflected as a decrease in  $n_s$ . Comparing the relative strength of the  $(\pi, 0)$  peak with and without Zn, it is hard to say that the data points towards this conclusion. The optical data from pure and Zn doped samples may provide a possible explanation for this. In Zn free samples, the Drude weight shifts to the delta function at  $\omega=0$  when cooled below  $T_c$ . In Zn doped samples, on the other hand, some of the Drude weight does not go to zero frequency but instead stays at a very small frequency [61]. This means that weight at the delta function will be smaller in Zn doped samples. With our energy resolution, however, we cannot distinguish this change of superfluid density. Furthermore, one should compare samples with the same  $\delta$ , and that has been a hard parameter to control in the growth of Bi2212. It should be noted that while we have included this for the sake of discussion, the role of Zn forming local moments in underdoped cuprates is still an open issue [62].

The third issue concerns the spectral lineshape of the photoemission experiments. The systematic changes in ARPES data with Zn doping provide a new perspective on several long standing problems about the unusual pho-

toemission lineshape observed in high  $T_c$  superconductors. These problems can best be illustrated by the spectral lineshape change at  $(\pi, 0)$  above and below  $T_c$ , as shown in Fig. 3. As the temperature is lowered below  $T_c$ , a sharp quasiparticle peak emerges at the low energy edge of the broad normal state feature accompanied by a dip structure at higher energy. In Zn-Bi2212 the dip is gone, but the peak persists and even gains intensity as it is broadened but with roughly similar height. It is often assumed that the sharp peak develops below  $T_c$  because of an increase in quasiparticle lifetime, which is independently measured in other experiments [63] [64]. The traditional interpretation of the peak and dip structure is associated with the electronic pairing mechanism [65]. In this case, the peak is the superconducting quasiparticle at gap energy  $\Delta$  (for the case when the normal state quasiparticle peak is at the Fermi level) and the dip is caused by the suppression of the spectral weight between the energy  $\Delta$  and  $3\Delta$  as the electronic medium itself is gapped. More recently, a phenomenological self-energy was proposed to explain the peak and the dip in a very similar spirit [66]. In both of these cases, the dip and the peak go hand in hand because they are manifestations of the same self-energy change.

The data from Zn-Bi2212 add to a list of puzzles associated with the above interpretation as Zn doping kills the dip without diminishing the intensity of the peak so that the peak and dip do not necessarily have follow each other. The other puzzles are represented by the following examples. First, the expectation of spectral weight suppression between  $\Delta$  and  $3\Delta$  is based on a very general argument compatible with any electronic pairing mechanism so that the dip will appear as long as the electronic excitation spectrum opens a gap. This expectation is in strong contrast to the fact that one does not see a dip structure in the pseudogap state of the underdoped samples where the electronic excitation spectrum opens a gap [26]. It is also very strange that the sharp peak emerges only below  $T_c$  in the underdoped samples although the spectrum is gapped well above  $T_c$ , as if the single particle spectral function is sensitive to the superconducting order. Further, the intensity of the sharp peak shows a monotonic correlation with doping and, thus, the superfluid density. These empirical observations are not compatible with the conventional wisdom that the single particle spectral function should not be sensitive to the superconducting condensate. In fact, we believe this puzzle is a very important clue and its understanding will lead to a deeper insight into these materials. Second, the sharp peak and the broad feature at higher binding energy side of the dip seem to behave independently [67]. Fig. 3b shows the  $(\pi, 0)$  spectra in the superconducting state with different doping. It is clear that the energy of the superconducting peak hardly changes, but the broad feature and the shape of the dip changes significantly. Third, the photoemission spectra obtained in the normal

state of the doped superconductor show striking resemblance to that of the insulator, albeit the energy position of the broad feature near  $(\pi, 0)$  evolves with different doping. Finally, we have to worry about the fact that the peak and dip structures are not seen in YBCO. Despite the chain complication, we can still get the consistent result about the Fermi surface, the d-wave gap, and the sharp peak at X  $(\pi, 0)$  in YBCO [31]. However, the dip structure is not seen even in measurements where the sample is cleaved and kept at 10K continuously. More work is needed to connect the photoemission and tunnelling data of YBCO. We note a theoretical attempt to connect photoemission and tunnelling experimental data from Bi2212 [68].

The above puzzles suggest that we may need to re-evaluate the problem in a very different way, as the conventional wisdom is wanting. The finding in the Zn doped samples reinforced our concern whether a quasiparticle picture with a certain form of the self-energy is the right approach to the problem. The question whether one should start with a quasiparticle approach lies at the heart of a long standing debate in the field [69] [70] [71] [72], following the early photoemission experiments [23]. It may be that the dip structure has an origin different from the  $\Delta$  to  $3\Delta$  suppression.

In conclusion, we recast the most important qualitative observation of our experiment - the destruction of the quasiparticle peak along  $\Gamma Y$  with relatively small amounts of Zn impurities. Whatever the microscopic mechanism causing the change, be it simple impurity scattering or some random pinning of the phase separated domains, this observation is significant to the understanding of the relevance of quasiparticles in the normal state. Data in Fig. 2a-b may reasonably be interpreted within the context of the quasiparticle picture, a concept that is the foundation of the modern theory of solids and is extensively used to address the high  $T_c$  problem. Yet, one would be very hard pressed to call the data in Fig. 2c-d as reflecting quasiparticles, and superconductivity with  $T_c$  as high as 78-83K survived. Taken naively, the existence of conventional quasiparticles with well defined  $\mathbf{k}$  does not seem to be necessary for the realization of high temperature superconductivity.

We acknowledge R. B. Laughlin, S.A. Kivelson, B. O. Wells, D. S. Dessau, M. Norman, A.J. Millis, A. Balatzky, A. Fujimori, D. J. Scalapino, H. Eisaki, and N. Nagosa for helpful discussions. ARPES experiments were performed at SSRL which is operated by the DOE Office of Basic Energy Science, Division of Chemical Sciences. The Office's Division of Material Science provided support for this research.

- [1] A. Maeda *et al.*, *Phys. Rev. B* **41**, 4112 (1990)
- [2] G. Xiao *et al.*, *Phys. Rev. B* **42**, 8752 (1990)
- [3] T.R. Chien, Z.Z. Wang, and N.P. Ong, *Phys. Rev. Lett.* **67**, 2088 (1991)
- [4] Y. Fukuzumi *et al.*, *Phys. Rev. Lett.* **76**, 684 (1996)
- [5] R. Lal *et al.*, *Phys. Rev. B* **49**, 6382 (1994)
- [6] T. Kluge *et al.*, *Phys. Rev. B* **52**, R727 (1995)
- [7] H. Hancotte *et al.*, *Phys. Rev. B* **55**, R3410 (1997)
- [8] H. Alloul *et al.*, *Phys. Rev. Lett.* **67**, 3140 (1991)
- [9] K. Ishida *et al.*, *Physica C (Amsterdam)* **179**, 29 (1991)
- [10] J.W. Loram, *Physica C* **235-240**, 134 (1994)
- [11] J.L. Tallon *et al.*, *Phys. Rev. Lett.* **79**, 5294 (1997)
- [12] D.A. Bonn *et al.*, *Phys. Rev. B* **50**, 4051 (1994)
- [13] K. Mizuhashi *et al.*, *Phys. Rev. B* **52**, R3884 (1995)
- [14] S. Tajima, R. Hauff, and W.-J. Jang, *SPIE* **2696**, 24 (1996)
- [15] C. Bernhard *et al.*, *Phys. Rev. Lett.* **77**, 2304 (1996)
- [16] H. Hirota *et al.*, *Physica B* **241-243**, 817 (1997)
- [17] K. Kakurai *et al.*, *Phys. Rev. B* **48**, 3485 (1993)
- [18] Y. Sidis *et al.*, *Phys. Rev. B* **53**, 6811 (1996)
- [19] J.M. Tranquada, cond-matt/9709325; J.M. Tranquada *et al.*, *Nature* **375**, 561 (1995)
- [20] K. Yamada *et al.*, *Phys. Rev. B* **57**, 6165 (1998); T. Suzuki *et al.*, *Phys. Rev. B* **57**, R3229 (1998); H. Kimura *et al.*, preprint
- [21] N.L. Wang *et al.*, *Phys. Rev. B* **57**, R11081 (1998)
- [22] Y. Koike *et al.*, *Solid State Communication* **82**, 889 (1992); Y. Koike *et al.*, *Physica C* **282-287**, 1233 (1997); Y. Koike *et al.*, *Journal of Low Temp. Phys.* **105**, 317 (1996); M. Akoshima *et al.*, *Phys. Rev. B* **57**, 7491 (1998)
- [23] C.G. Olson *et al.*, *Science* **245**, 731 (1989)
- [24] Z.-X. Shen *et al.*, *Phys. Rev. Lett.* **70**, 1553 (1993)
- [25] D.S. Marshall *et al.*, *Phys. Rev. Lett.* **76**, 4841 (1995)
- [26] A.G. Loeser *et al.*, *Science* **273**, 325 (1996)
- [27] H. Ding *et al.*, *Nature* **382**, 51 (1996)
- [28] P.J. White *et al.*, unpublished
- [29] C. Quitmann *et al.*, *Phys. Rev. B* **53**, 6819 (1996); C. Quitmann *et al.*, *Journal of Superconductivity* **8**, 635 (1995); P. Almeras *et al.*, *Solid State Communications* **91**, 535 (1994); P. Almeras *et al.*, *Physica C* **235-240**, 957 (1994)
- [30] C. Gu *et al.*, *J. Phys. Chem. Solids* **54**, 1177 (1993)
- [31] M.C. Schabel *et al.*, *Phys. Rev. B* **55**, 2796 (1997); M.C. Schabel *et al.*, *Phys. Rev. B* **57**, 6107 (1998); M.C. Schabel *et al.*, *Phys. Rev. B* **57**, 6090 (1998)
- [32] In this paper we follow the conventional notation in the literature and call the broad peak seen in the normal state the quasiparticle peak. More critical analysis of the normal state data, especially the contrast between the normal and superconducting states at  $(\pi, 0)$ , suggests that one may not be able to meaningfully describe a quasiparticle peak in the normal state, at least for the  $\mathbf{k}$ -space region away from the  $(0,0)$  to  $(\pi, \pi)$  line. (G.A. Sawatzky, private communication)
- [33] R. Yoshizaki *et al.*, *J. Low Temp. Phys.* **105**, 927 (1996); D.-S. Jeon *et al.*, *Physica C* **253**, 102 (1995); L.-X. Chen, H. Ikeda, and R. Yoshizaki, *Physica C* **282-287**, 1205 (1997)
- [34] G.D. Gu *et al.*, *J. Crystal Growth* **137**, 472 (1994); G.D. Gu *et al.*, *J. Crystal Growth* **130**, 325 (1993); G.D. Gu *et al.*, *Physica C* **263**, 180 (1996)

- [35] M. Randeria *et al.*, *Phys. Rev. Lett.* **74**, 4951 (1995)
- [36] H. Ding *et al.*, *Phys. Rev. Lett.* **78**, 2628 (1997)
- [37] The low temperature data does allow the possibility of a gap, but more needs to be done before a conclusion can be drawn.
- [38] D.S. Dessau *et al.*, *Phys. Rev. Lett.* **66**, 2160 (1991)
- [39] Y. Hwu *et al.*, *Phys. Rev. Lett.* **67**, 2573 (1991)
- [40] V.J. Emery, S.A. Kivelson, O. Zachar, *Phys. Rev. B* **56**, 6120 (1997)
- [41] V.J. Emery, S.A. Kivelson, *Nature* **374**, 4347 (1995)
- [42] S. Doniach, M. Inui, *Phys. Rev. B* **41**, 6668 (1990)
- [43] C.S. de Melo, M. Randeria, J.R. Engelbrecht, *Phys. Rev. Lett.* **71**, 3202 (1993)
- [44] K. Morikawa *et al.*, *Phys. Rev. B* **54**, 8446 (1996)
- [45] M. Hase *et al.*, *J. Magn. Magn. Mat.* **177-181**, 611 (1998)
- [46] K. Manabe *et al.*, *Phys. Rev. B* **58**, R575 (1998)
- [47] T. Sekine *et al.*, *J. Phys. Soc. Japan* **67**, 1440 (1998)
- [48] M. Akoshima *et al.*, *Phys. Rev. B* **57**, 7491 (1998)
- [49] R. Liu *et al.*, *Phys. Rev. B* **45**, 5614 (1992); R. Liu *et al.*, *Phys. Rev. B* **46**, 11056 (1992)
- [50] J.M. Harris *et al.*, *Phys. Rev. B* **54**, R15665 (1996)
- [51] K. Gofron *et al.*, *Phys. Rev. Lett.* **73**, 3302 (1994)
- [52] B.O. Wells *et al.*, *Phys. Rev. Lett.* **74**, 964 (1995)
- [53] A. Ino *et al.*, cond-mat/9809311
- [54] E. Dagatto, *Rev. Mod. Phys.* **66**, no. 3, 763 (1994)
- [55] C. Kim, *et al.*, *Phys. Rev. Lett.* **80**, 4245 (1998)
- [56] T. Tokyama and S. Maekawa, private communication
- [57] D. Poilblanc, D.S. Scalapino, W. Hanke, *Phys. Rev. Lett.* **72**, 884 (1994)
- [58] A. V. Mahajan *et al.*, *Phys. Rev. Lett.* **72**, 3100 (1994)
- [59] C. Pepin and P. A. Lee, *Phys. Rev. Lett.* **81**, 2779 (1998)
- [60] B. Nachumi *et al.*, *Phys. Rev. Lett.* **77**, 5421 (1996)
- [61] D.N. Basov, B. Dabrowski, and T. Timusk, *Phys. Rev. Lett.* **81**, 2132 (1998)
- [62] G. V. M. Williams and J. L. Tallon, *Phys. Rev. B* **57**, 10984 (1998); C. Bernhard *et al.*, *Phys. Rev. Lett.* **58**, R8937 (1998)
- [63] D.A. Bonn, *et al.*, *Phys. Rev. Lett.* **68**, 2390 (1992)
- [64] J.M. Harris, *et al.*, *J. Low Temp. Phys.* **105**, 877
- [65] P.B. Littlewood and C. M. Varma, *Phys. Rev. B* **45**, 12636 (1992)
- [66] M.R. Norman and H. Ding, *Phys. Rev. B* **57**, R11089 (1998)
- [67] Empirically, one may naively think that the peak and dip minimum energy actually scale with each other. This is reasonable as the dip minimum energy is basically determined by the peak energy and half of the width.
- [68] M. Franz and A.J. Millis, cond-mat/9805401
- [69] P.W. Anderson and Y. Ren, *High  $T_c$  Superconductivity Proceedings Los Alamos Symposium 1989*, eds. K. S. Bedell *et al.* (Addison-Wesley)
- [70] G.A. Sawatzky, *Nature* **342**, 480 (1989)
- [71] M.I. Salkola, V. J. Emery, and S. A. Kivelson, *Phys. Rev. Lett.* **77**, 155 (1996)
- [72] L.B. Ioffe and A.J. Millis, cond-mat/9801092

$\text{Bi}_2\text{Sr}_2\text{Ca}(\text{Cu}_{1-x}\text{Zn}_x)_2\text{O}_{8+\delta}$   $\mathbf{H} \parallel c\text{-axis}$  Zero Field Cooled

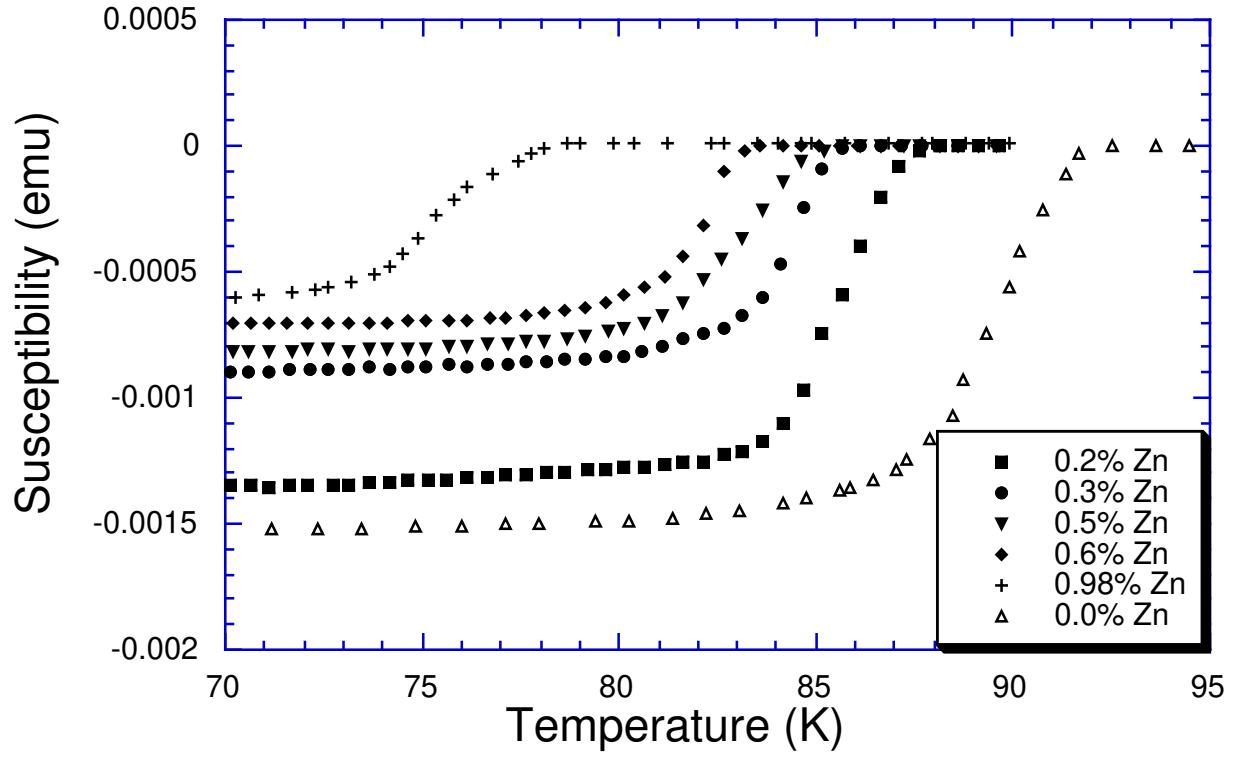


FIG. 1. Susceptibility measurements for various concentrations of  $\text{Bi}_2\text{Sr}_2\text{Ca}(\text{Cu}_{1-x}\text{Zn}_x)_2\text{O}_{8+\delta}$  samples. The inset provides the symbol legend.



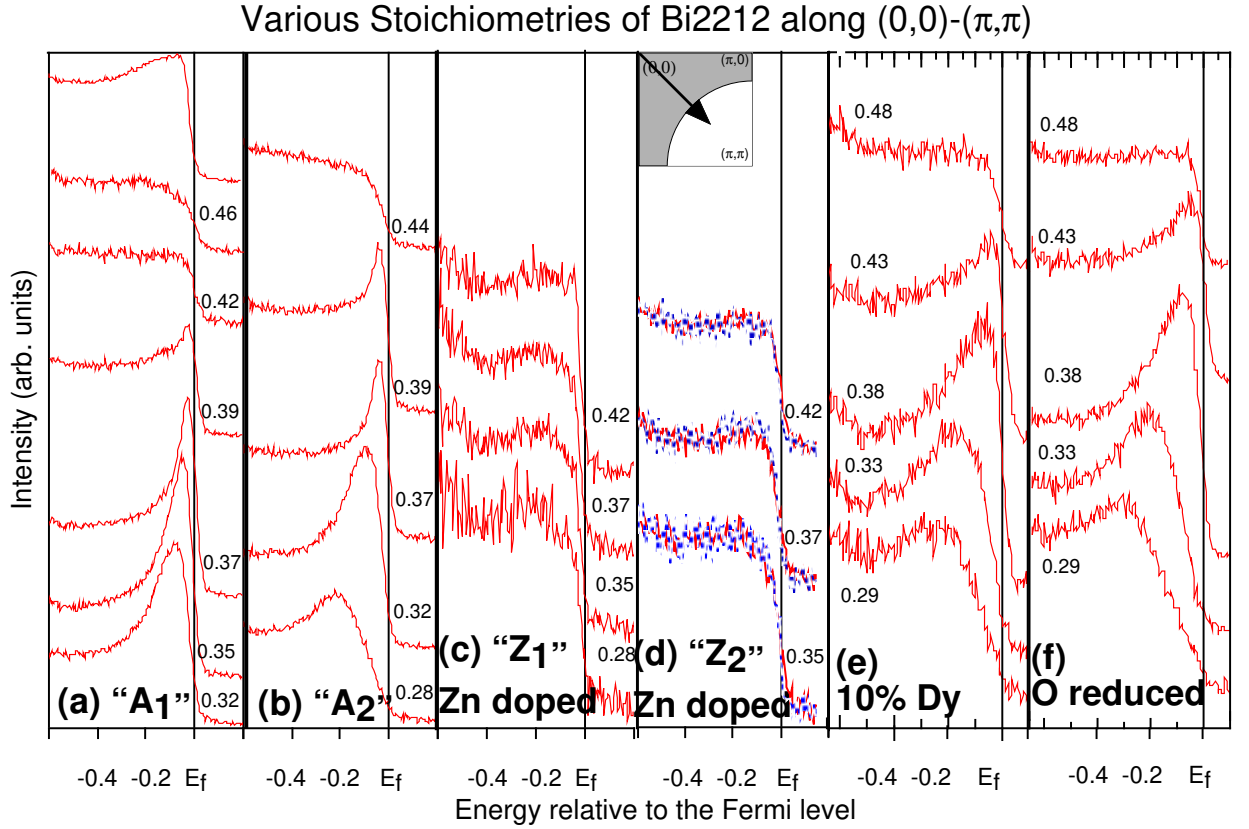


FIG. 2. ARPES data along (0,0) to ( $\pi,\pi$ ) cut in pure  $\text{Bi}_2\text{Sr}_2\text{CaCu}_2\text{O}_{8+\delta}$  with  $T_c$  of 91K (a and b),  $\text{Bi}_2\text{Sr}_2\text{Ca}(\text{Cu}_{1-x}\text{Zn}_x)_2\text{O}_{8+\delta}$  with  $T_c$  of 83K (c and d), 10% Dy doped  $\text{Bi}_2\text{Sr}_2(\text{Ca}_{1-x}\text{Dy}_x)\text{Cu}_2\text{O}_{8+\delta}$  with  $T_c$  of 65K (underdoped sample) (e), and oxygen reduced  $\text{Bi}_2\text{Sr}_2\text{CaCu}_2\text{O}_{8+\delta}$  with  $T_c$  of 67K (f). All spectra were collected at 100K under comparable conditions. The number marks the distance away from the  $\Gamma$  to ( $\pi,\pi$ ) line. For the Zn doped sample, spectra recorded below  $T_c$  (broken line) is the same within the experimental uncertainty. The top curve in Panel (a) is the *average* of the other curves in the panel.

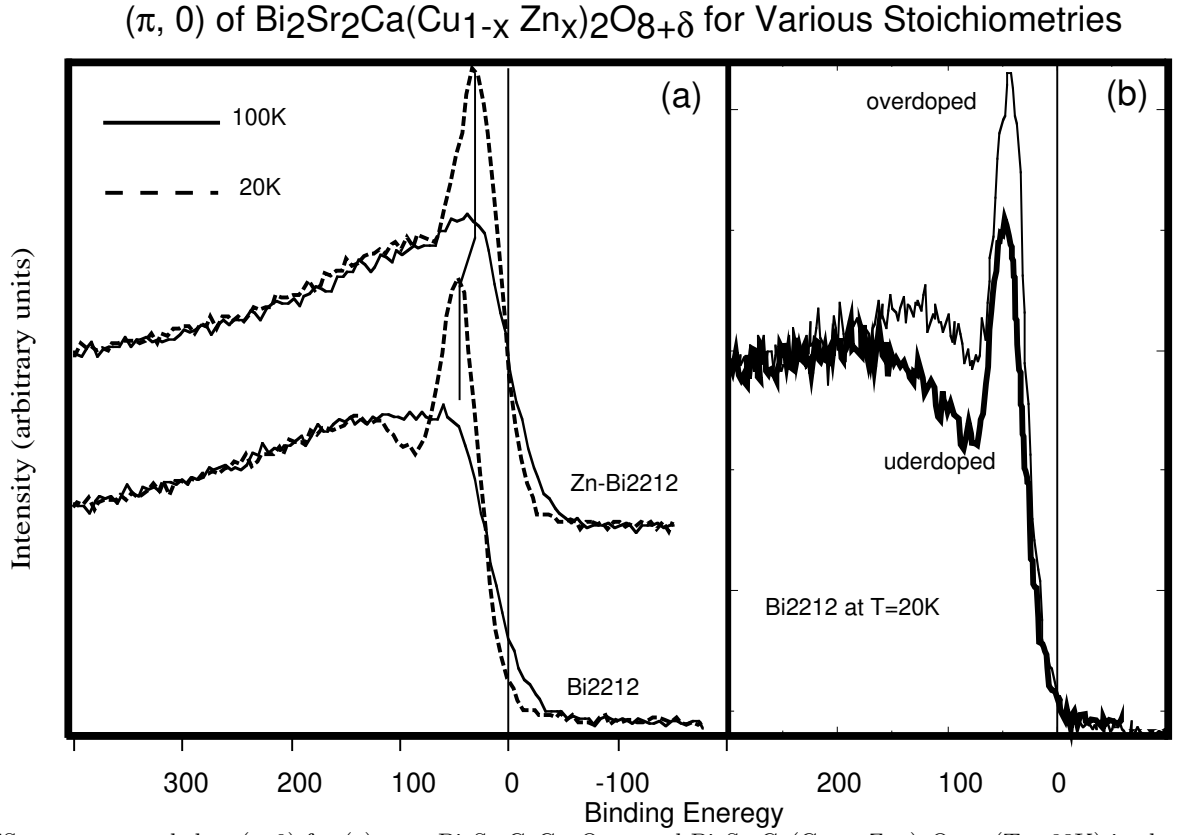


FIG. 3. ARPES spectra recorded at  $(\pi, 0)$  for (a) pure  $\text{Bi}_2\text{Sr}_2\text{CaCu}_2\text{O}_{8+\delta}$  and  $\text{Bi}_2\text{Sr}_2\text{Ca}(\text{Cu}_{1-x}\text{Zn}_x)_2\text{O}_{8+\delta}$  ( $T_c \approx 83\text{K}$ ) in the normal and superconducting states. The dashed line is data recorded at 20K, and the solid line is data recorded at 100K and (b) for underdoped and overdoped pure  $\text{Bi}_2\text{Sr}_2\text{CaCu}_2\text{O}_{8+\delta}$ .